

RSC Advances



This is an *Accepted Manuscript*, which has been through the Royal Society of Chemistry peer review process and has been accepted for publication.

Accepted Manuscripts are published online shortly after acceptance, before technical editing, formatting and proof reading. Using this free service, authors can make their results available to the community, in citable form, before we publish the edited article. This *Accepted Manuscript* will be replaced by the edited, formatted and paginated article as soon as this is available.

You can find more information about *Accepted Manuscripts* in the [Information for Authors](#).

Please note that technical editing may introduce minor changes to the text and/or graphics, which may alter content. The journal's standard [Terms & Conditions](#) and the [Ethical guidelines](#) still apply. In no event shall the Royal Society of Chemistry be held responsible for any errors or omissions in this *Accepted Manuscript* or any consequences arising from the use of any information it contains.

COMMUNICATION

Controlled Formation of Nanoparticle Clusters Mediated by Electrostatic Interaction

Cite this: DOI: 10.1039/x0xx00000x

Xiaoshuang Shen*, Chao Mei, Yuxue Zhou, Weiwei Xia, Min Zhou and Xianghua Zeng*

Received 00th January 2012,

Accepted 00th January 2012

DOI: 10.1039/x0xx00000x

www.rsc.org/

Nanoparticle clusters are usually referred to as colloidal molecules due to their composition, configuration and gap dependent properties. Here, we report a general strategy for high yield fabrication of homo- and hetero- nanoparticle clusters on substrate with controlled configuration and gap through a self-assembly process mediated by electrostatic interaction.

Nanoparticles (NPs) are often regarded as artificial atoms due to their size- and shape-dependent properties.¹ These artificial atoms can further form clusters with well-defined stoichiometry and configuration of constituent NPs, the so-called artificial molecules.² Novel collective properties usually emerge in NP clusters owing to the electric and magnetic couplings between adjacent NPs.^{3,4} A well-known case is the plasmonic molecules,^{5,6} in which some interesting physical phenomena, such as magnetic dipole and Fano resonances, were observed.^{7,8} By controlling the number and configuration of the constituent NPs, as well as the inter-particle gaps, the collective properties of NP clusters can be highly controlled and optimized for various applications,⁹ such as surface-enhanced Raman scattering (SERS)¹⁰, optical sensing,¹¹ and medical diagnosis.¹²⁻¹⁴

Several methods have been developed to fabricate NP clusters by exploiting random aggregation,¹⁵ hydrophobic interaction,¹⁶ and chemical linkers (e.g., DNA molecules).^{17,18} However, the success of these methods was mainly limited in fabrication of the homo- NP dimers. Although more complex NP clusters can be synthesized by using DNA as linkers, it suffers from complex procedure and materials specific. Compared to homo- NP clusters, hetero- NP clusters,¹⁹⁻²¹ which are composed of NPs with different shapes or even compositions, attract more and more attention due to the hybridization of the properties among different kinds of NPs, which can bring new possibilities in the chemical and physical properties. In this respect, an effective method is lacking.

Here, we report a new strategy for high yield fabrication of homo- and hetero- NP clusters on substrate through a self-assembly process mediated by electrostatic interaction. The strategy utilizes the unique characteristic of electrostatic interaction: once a charged NP attaches to an oppositely charged one, the attaching of another same charged NP to the formed NP cluster will be inhibited due to the electrostatic repulsion among the same charged NPs. This characteristic,

combining with the using of substrate, makes it feasible to precisely control the stoichiometry and configuration of the constituent NPs in the formed clusters. Furthermore, diblock copolymer is successfully exploited as a shell to tune the NP gap distance from a few nanometers to more than ten nanometers. Since a variety of NPs, including metal, magnetic and luminescence NPs, can be encapsulated in diblock copolymer shells,^{22,23} the strategy described here can serve as a general method towards homo- and hetero- NP clusters with controllable NP gap distance.

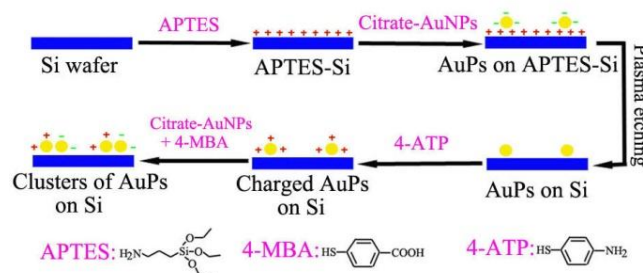


Figure 1. Schematics for fabrication of NP clusters mediated by electrostatic interaction.

Figure 1 depicts the schematics of the fabrication process. First, citrate-stabilized Au NPs were deposited onto a substrate functionalized by 3-aminopropyltriethoxysilane (APTES). It is known that citrate-stabilized Au NPs are negatively charged, while APTES makes the substrate positively charged. When the substrate functionalized by APTES was immersed into the solution containing citrate-stabilized Au NPs, the Au NPs can stick to the substrate through electrostatic attraction. The distribution density of Au NPs on substrate can easily be controlled by changing the immersion time and the concentration of Au NPs in solution. According to our observations, the distribution density of Au NPs on substrate is more sensitive to the concentration of Au NPs in solution. Then plasma etching was used to remove the APTES and citrate, leaving bare Au NPs on substrate. The use of substrate here makes it easier to modify Au NP surfaces with various functional molecules in the next step, and it does not need to worry about the aggregation of NPs which usually happens when modifying NPs in solution. After modifying Au NPs with 4-aminothiophenol (4-ATP) molecules, we immersed

the substrate into the solution containing citrate-stabilized Au NPs again. Although the 4-ATP molecules make the Au NPs on substrate positively charged, it is found that the electrostatic interaction between these NPs and the negatively charged NPs in solution is too weak to bind them together. It is known that the attractive interactions mediating the self-assembly must be strong enough to overcome the entropic "penalty" associated with the loss of translational/rotation degrees of freedom upon NP aggregation.²⁴

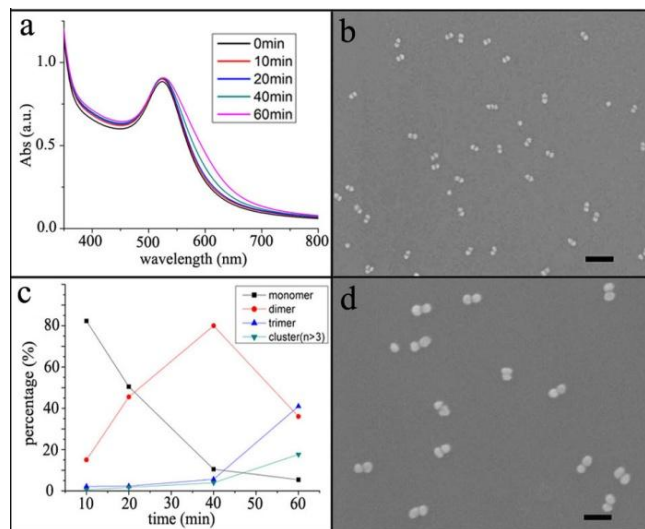


Figure 2. (a) UV-vis spectra of Au NP solution after addition of 4-MBA; (b) SEM image of dimers of 15-nm Au NPs; (c) yields of different NP cluster with different immersion time; (d) SEM image of dimers of 30-nm Au NPs. Scale bars in (b) and (d) represent 100 nm.

To solve this problem, a certain amount of 4-mercaptobenzoic acid (4-MBA) is added to the Au NP solution. The 4-MBA molecules can replace the citrate ions on the Au NP surfaces due to the strong interaction between thiol groups and Au. The replacement process was monitored by UV-vis extinction spectra (Figure 2a). The slight shoulder which gradually appeared at about 600 nm is characteristic of reduced inter-particle interactions and electromagnetic coupling between NPs.²⁵ The replacement of citrate ions by 4-MBA molecules gives rise to the hydrophobic interaction between solution (water) and Au NPs due to the hydrophobic groups (phenyl) of 4-MBA molecules, which will increase the internal energy of the system, and in proper experimental conditions, the decrease of internal energy in the formation of a cluster can be large enough to overcome the entropic "penalty".

Figure 2b shows a SEM image of the sample obtained through immersing the substrate into the Au nanoparticle solution with freshly added 4-MBA for 40 minutes, and about 80% of the clusters are dimers of 15-nm Au NPs. It is easy to monitor the self-assembly process due to the use of substrate, because we can suspend the self-assembly process at any time by taking the substrate out of the solution. This advantage is very useful for us to optimize the yield of dimers, which is a function of time. We found that when the immersion time is 20 minutes, only about 30% of the clusters are dimers, and most of the products are single NPs (Figure 2c). On the other hand, if the immersion time is increased to 60 minutes, the percentage of dimers is about 35%, accompanying with ~40% trimers (Figure 2c). Further increasing the immersion time results in the increase of percentage of clusters containing more than three particles, and the number of NPs within a cluster becomes uncontrollable. It is clear that at the early stage, formation of dimers is the main process, which indicates electrostatic interaction

dominates the assembly process, while at the later stage, the tendency of decreasing the surface energy becomes prevailing due to the increasing of covering of 4-MBA on Au NP surfaces. In this case, formation of large clusters is favorable. The key point for high-yield fabrication of NP dimers is to make the self-assembly process under the control of electrostatic interaction.

This method can be directly used to fabricate dimers of Au NPs of other sizes, as long as proper amount of 4-MBA and immersion time are chosen, which depends on the specific solution property. For example, when 30-nm Au NP solution are used, more amount of 4-MBA is needed to make these nanoparticles unstable in solution, and 30-nm Au NP dimers also can be obtained with a high yield (Figure 2d).

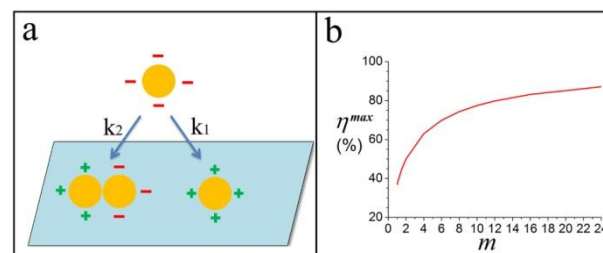


Figure 3. (a) Schematic for attaching a negative NP to an individual positive NP or to a NP dimer on the substrate. The rates of these two processes are different (k_1 vs. k_2); (b) The relation between the ratio of k_1 and k_2 (m) and the maximal yield of the dimers (η^{max}).

The electrostatic repulsion among the same charged NPs plays a crucial role in the high-yield formation of NP dimers. If the electrostatic repulsion is negligible, thus the rates of attaching a negative NP in solution to the formed NP dimer and to the individual NP on the substrate can be taken the same (Figure 3a. For more discussion about this and the detailed deduction of the following equations, see ESI.). In this case, the number of the dimers, denoted by N_d , can be found as a function of time, t ,

$$N_d(t) = N_0 k t e^{-kt},$$

where k is the rate of attaching a particle to the NP dimers or to the individual NPs, and N_0 is the initial number of individual NPs on the substrate. It can be easily proved that the maximal yield of dimers is

$$\eta^{max} = \frac{N_d^{max}}{N_0} = e^{-1} \approx 36.8\%,$$

which is much lower than that observed in our experiments. If the electrostatic repulsion can effectively decrease the rate of attaching a NP to the formed dimers, the function $N_d(t)$ will be modified to

$$N_d(t) = k_1 N_0 \frac{e^{-k_1 t} - e^{-k_2 t}}{k_2 - k_1},$$

where k_1 and k_2 are the rates of attaching a NP to the individual NPs and to the NP dimers, respectively. In this case, the maximal yield of NP dimers will turn out to be

$$\eta^{max} = \frac{N_d^{max}}{N_0} = \frac{m}{m-1} \left(\frac{1}{m^{m-1}} - \frac{1}{m} \right),$$

where m represents k_1 / k_2 . The relation between η^{max} and m is pictured at Figure 3b. When m tends to 1, the η^{max} tends to 36.8% as expected. To increase the η^{max} to about 80%, the value of m should be as large as 12 (For $m = 12$, $\eta^{max} = 79.78\%$). Thus in our experiments, the rate of attaching a NP to an individual NPs is much larger than that of attaching a NP to a NP dimer, which can be

attributed to the electrostatic repulsion between the same charged NPs in the dimers. The role of electrostatic repulsion will be demonstrated again in the following experiments about heterodimers.

To fabricate heterodimers using 15-nm and 30-nm Au NPs as building blocks, there are two ways that can be chosen. We can deposit 15-nm Au NPs on substrate first and then stick 30-nm Au NPs to them, or use an opposite process. Using the former way, the heterodimers can be obtained with an extremely high yield (~90%), as shown in Figure 4a. Once a large NP sticks to a small one, the electrostatic repulsion among the large NPs can effectively prevent the attaching of another large one to the formed heterodimer. Using the latter way, the yield of heterodimers is sensitive to the immersion time. Figure 4b shows the products obtained with immersion time of 20 minutes, and about 60% of clusters are heterodimers. In the products, some percentages (~15%) of heterotrimers also can be observed. It is noteworthy that these heterotrimers take a liner configuration in which two small NPs are on the opposite sides of a large NP. Obviously, it is a result of the repulsion between the two small NPs. The yield of the heterotrimers can be increased to above 60% when the immersion time is extended to 40 minutes (Figure 4c). Most of these heterotrimers also take a liner configuration, and almost none of heterotrimers with triangular configuration can be found. Some heterotrimers deviate from the ideal liner configuration, and it is likely due to the non-spherical shape of the 30-nm Au NPs. These results clearly demonstrate that it is electrostatic interaction rather than other interaction, dominates the self-assembly process.

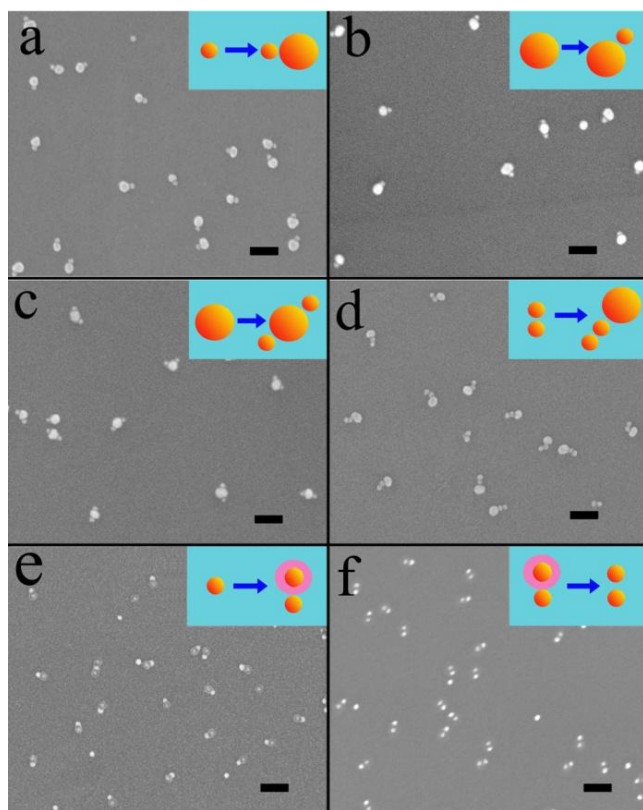


Figure 4. SEM images of heterodimers (a, b) and heterotrimers (c, d). The insets show the schematics of corresponding self-assembly process. (e) SEM image of the NP dimers with two NPs separated by a layer of PS-PAA shell; (f) SEM image of the NP dimers with about 8 nm gap distance after removing the polymer shell by plasma etching. The scale bars represent 100 nm.

It is useful to fabricate NP clusters with different configuration due to their structure-dependent properties. To fabricate another type

of heterotrimers, where the two small NPs are contacted, we start with a substrate with dimers of 15-nm Au NPs on it and then stick 30-nm Au NPs to the dimers. Figure 4d shows a SEM image of the obtained heterotrimers. These heterotrimers do not have the central symmetry possessed by that shown in Figure 4c. The ability of fabricating NP clusters with different symmetry, which may possess different plasmonic properties, is useful for their applications.

Besides the configuration, another key factor which influences the cluster properties is the gap distance between NPs. For the clusters described above, the NP gap distance is intrinsically determined by the length of ligands, i.e. the 4-MBA and 4-ATP molecules, which is about 1~2 nanometers. In principle, one can tune the gap distance by altering the ligands used. Here, we use another type of organic molecules to tune the gap distance in a larger range. As demonstrated by several groups, diblock copolymers can form a shell with thickness ranging from several nanometers to tens of nanometers on NP surfaces, resulting in core@shell NPs. If we can make one of the core-shell NPs stick to an un-coated NP on substrate, the dimers obtained will have a highly tunable particle gap distance, which depends on the molecular weight of the diblock copolymer used.

Polystyrene-*b*-poly(acrylic acid) (PSPAA, M_n of PS: 154, M_n of PAA: 49) is used to encapsulate Au NPs, which makes these NPs negatively charged. When the substrate with positively charged Au NPs (modified with 4-ATP) on it is immersed into the solution containing Au@PSPAA core@shell NPs, the same as in the above cases, we also meet with the problem of how to overcome the entropy penalty. However, increasing the interaction through the ligand-exchange previously used does not work in this case due to the coverage of PSPAA on Au NP surfaces. To overcome the entropy penalty, an alternative way is to decrease the system entropy itself. The Au@PSPAA core@shell NPs are very stable in aqueous solution because of the electrostatic and steric repulsion arising from the polymer shell, which makes it possible to obtain high concentration of Au@PSPAA core@shell NPs in solution without aggregation of these NPs. It is known that higher volume fraction of NPs in solution means lower free volume because less free space is available for each NP to perform translational and rotational movement.

Solvent evaporation is used to achieve high concentration of Au@PSPAA core@shell NPs, towards which, 25 μ L of Au@PSPAA core@shell NP solution is dropped onto the substrate which is pre-placed in a vial. Then the vial is covered by a glass slide to slow down the evaporation rate, which can effectively suppress the compensation flow in the droplet arising from solvent evaporation, and thus avoid the formation of “coffee ring” pattern on substrate.²⁶ When the solution was left about 1~2 μ L, remove it with a pipette and rinse the substrate with water. As shown in Figure 4e, most of the Au@PSPAA core@shell NPs selectively stick to 4-APT modified Au NPs with one-to-one manner, leading to the formation of dimers with two NPs separated by a layer of PSPAA shell. After removing the PSPAA shell by plasma etching, Au NP dimers with gap distance equal to the thickness of PSPAA shell, which is about 8 nm here, are obtained (Figure 4f). The nanoparticle clusters prepared here have simple two-dimensional geometries, and the removing of the polymer shell does not cause any changes of their structure. The gap distance can be easily tuned through changing the shell thickness. For example, if PS(404)PAA(62) is used, dimers with gap distance about 15 nm can be fabricated (Figure S1). Besides controlling the gap distance, using polymer shell has another advantage. The method does not depend on the properties of NPs encapsulated in polymer shells, so it can serve as a general method to fabricate homo- and hetero- NP dimers since a variety of NPs can be encapsulated in polymer shell. As a demonstration, Au-Fe₂O₃

heterodimers are fabricated through encapsulating Fe₂O₃ NPs in polymer shell and then sticking the core@shell NPs to Au NPs on substrate (Figure S2).

Compared to the method based on self-assembly of colloidal NPs, optical and electron beam lithography can be served as a more controllable method for fabrication of NP clusters on substrate in any two-dimensional geometry with uniformity of particle sizes and periodicity.^{27,28} However, the self-assembly of colloid NPs provides a versatile and low-cost route to the formation of NP clusters. Many kinds of NPs with different shape and composition are available by virtue of the development of colloidal synthesis techniques, which can be used as building blocks to fabricate NP clusters. Especially in fabrication of NP clusters with compositional asymmetry, tunable sub-10 nm gap distance, and three-dimensional geometries, the self-assembly method shows obvious superiority over the lithography method.

Conclusions

In conclusion, a facile and general method is developed for high yield fabrication of home- and hetero- NP clusters on substrate through a self-assembly process mediated by electrostatic interaction. The electrostatic repulsion among the same charged NPs sufficiently decreases the rate of attaching a NP in solution to the NP dimers on substrate, and thus increases yield of NP dimers. The electrostatic repulsion among the same charged NPs also leads to the formation of heterotrimers with linear configuration. Furthermore, diblock copolymer was successfully exploited as a shell to tune the NP gap distance from a few nanometers to more than ten nanometers. The fabrication method reported here will benefit the applications of NP clusters.

Notes and references

School of Physical Science and Technology & Institute of Optoelectronic Technology, Yangzhou University, Yangzhou 225002, P. R. China

* Corresponding author. E-mail:

xsshen@yzu.edu.cn; xhzeng@yzu.edu.cn.

Acknowledgements

The work was funded through the Natural Science Foundation of the Jiangsu Higher Education Institutions of China (No. 14KJB150028), Natural Science Foundation of China (No.61474096) and Natural Science Foundation of China for the Youth (No.21101135 and No. 61301026). The authors thank Professor Hongyu Chen in NTU for helpful discussion about the experimental results.

Electronic Supplementary Information (ESI) available: Experimental procedure, theoretical analysis of the NP dimer yield and Fig. S1–S2. See DOI: 10.1039/c000000x/

- U. Banin, Y. Cao, D. Katz and O. Millo, *Nature*, 1999, **400**, 542.
- H. Wang, D. W. Brandl, P. Nordlander and N. J. Halas, *Accounts Chem. Res.*, 2007, **40**, 53.
- Z. Zhu, J. Guo, W. Liu, Z. Li, B. Han, W. Zhang and Z. Tang, *Angew. Chem. Int. Ed.*, 2013, **52**, 13571.
- T. Zhou, B. Dong, H. Qi, H. K. Laua and C. Y. Li, *Nanoscale*, 2014, **6**, 4551.
- X. Shen, P. Zhan, A. Kuzyk, Q. Liu, A. Asenjo-Garcia, H. Zhang, F. J. G. de Abajo, A. Govorov, B. Ding and N. Liu, *Nanoscale*, 2014, **6**, 2077.
- H. Chen, L. Shao, Q. Li and J. Wang, *Chem. Soc. Rev.*, 2013, **42**, 2679.
- J. A. Fan, C. Wu, K. Bao, J. Bao, R. Bardhan, N. J. Halas, V. N. Manoharan, P. Nordlander, G. Shvets and F. Capasso, *Science*, 2010, **328**, 1135.
- Z. Yang, Z. Hao, H. Lin and Q. Wang, *Nanoscale*, 2014, **6**, 4985.
- J. Gong, G. Li and Z. Tang, *Nano Today*, 2012, **7**, 564.
- C. Dong, Z. Yan, J. Kokx, D. B. Chrisey and C. Z. Dinu, *Appl. Surf. Sci.*, 2012, **258**, 9218.
- S. Liu and Z. Tang, *J. Mater. Chem.*, 2010, **20**, 24.
- C. Bhattacharya, Z. Yu, M. J. Rishel and S. M. Hecht, *Biochem.*, 2014, **53**, 3264.
- Z. Yu, R. M. Schmaltz, T. C. Bozeman, R. Paul, M. J. Rishel, K. S. Tsosie and S. M. Hecht, *J. Am. Chem. Soc.*, 2013, **135**, 2883.
- P. Miao, B. Wang, Z. Yu, J. Zhao and Y. Tang, *Biosens Bioelectron.*, 2014, **63C**, 365.
- G. Chen, Y. Wang, L. H. Tan, M. Yang, L. S. Tan, Y. Chen and H. Chen, *J. Am. Chem. Soc.*, 2009, **131**, 4218.
- A. S. Urban, X. Shen, Y. Wang, N. Large, H. Wang, M. W. Knight, P. Nordlander, H. Chen, and N. J. Halas, *Nano Lett.*, 2013, **13**, 4399.
- A. Samanta, Z. Deng and Y. Liu, *Nanoscale*, 2014, **6**, 4486.
- S. J. Tan, M. J. Campolongo, D. Luo and W. Cheng, *Nature Nanotech.*, 2011, **6**, 268.
- M. Frederiksen and D. S. Sutherland, *Nanoscale*, 2014, **6**, 731.
- J. Zhu, Y. Lu, Y. Li, J. Jiang, L. Cheng, Z. Liu, L. Guo, Y. Pan and H. Gu, *Nanoscale*, 2014, **6**, 199.
- L. V. Brown, H. Sobhani, J. Lassiter, P. Nordlander and N. J. Halas, *ACS Nano*, 2010, **4**, 819.
- H. Wang, L. Chen, Y. Feng and H. Chen, *Accounts Chem. Res.*, 2013, **46**, 1636.
- T. Chen, M. X. Yang, X. J. Wang, L. H. Tan and H. Y. Chen, *J. Am. Chem. Soc.*, 2008, **130**, 11858.
- K. J. M. Bishop, C. E. Wilmer, S. Soh and B. A. Grzybowski, *Small*, 2009, **5**, 1600.
- R. I. Michael, R. B. Heidi and J. H. Amanda, *ACS nano*, 2009, **3**, 386.
- R. D. Deegan, O. Bakajin, T. F. Dupont, G. Huber, S. R. Nagel and T. A. Witten, *Nature*, 1997, **389**, 827.
- J. Theiss, P. Pavaskar, P. M. Echernach, R. E. Muller and S. B. Cronin, *Nano Lett.*, 2010, **10**, 2749.
- T. Atay, J. H. Song and A. V. Nurmikko, *Nano Lett.*, 2004, **4**, 1627.